

4-2015

# Uncertainty in simulating gross primary production of cropland ecosystem from satellite-based models

Wenping Yuan

*Beijing Normal University, yuanwpcn@126.com*

Wenwen Cai

*Beijing Normal University*

Anthony L. Nguy-Robertson

*University of Nebraska-Lincoln*

Huajun Fang


*Chinese Academy of Sciences, Beijing, fanghj@igsnr.ac.cn*

Andrew E. Suyker

*University of Nebraska-Lincoln, asuyker1@unl.edu*

*See next page for additional authors*

Follow this and additional works at: <http://digitalcommons.unl.edu/natrespapers>

 Part of the [Agriculture Commons](#), [Environmental Monitoring Commons](#), [Oceanography and Atmospheric Sciences and Meteorology Commons](#), [Other Earth Sciences Commons](#), and the [Other Environmental Sciences Commons](#)

---

Yuan, Wenping; Cai, Wenwen; Nguy-Robertson, Anthony L.; Fang, Huajun; Suyker, Andrew E.; Chen, Yang; Dong, Wenjie; Liu, Shuguang; and Zhang, Haicheng, "Uncertainty in simulating gross primary production of cropland ecosystem from satellite-based models" (2015). *Papers in Natural Resources*. 520.  
<http://digitalcommons.unl.edu/natrespapers/520>

This Article is brought to you for free and open access by the Natural Resources, School of at DigitalCommons@University of Nebraska - Lincoln. It has been accepted for inclusion in Papers in Natural Resources by an authorized administrator of DigitalCommons@University of Nebraska - Lincoln.

---

**Authors**

Wenping Yuan, Wenwen Cai, Anthony L. Nguy-Robertson, Huajun Fang, Andrew E. Suyker, Yang Chen, Wenjie Dong, Shuguang Liu, and Haicheng Zhang

# Uncertainty in simulating gross primary production of cropland ecosystem from satellite-based models

Wenping Yuan,<sup>1</sup> Wenwen Cai,<sup>1</sup> Anthony L. Nguy-Robertson,<sup>2</sup> Huajun Fang,<sup>3</sup>  
Andrew E. Suyker,<sup>2</sup> Yang Chen,<sup>1</sup> Wenjie Dong,<sup>1</sup> Shuguang Liu,<sup>4</sup> Haicheng Zhang<sup>1</sup>

<sup>1</sup> State Key Laboratory of Earth Surface Processes and Resource Ecology, Beijing Normal University, Beijing 100875, China

<sup>2</sup> School of Natural Resources, University of Nebraska, Lincoln, NE 68583-0978, USA

<sup>3</sup> Key Laboratory of Ecosystem Network Observation and Modeling, Institute of Geographical Sciences and Natural Resources Research, Chinese Academy of Sciences, Beijing 100101, China

<sup>4</sup> State Engineering Laboratory of Southern Forestry Applied Ecology and Technology, Central South University of Forestry and Technology, Changsha, Hunan 410004, China

*Corresponding authors* — W. Yuan, email [yuanwpcn@126.com](mailto:yuanwpcn@126.com); H. Fang, email [fanghj@igsnr.ac.cn](mailto:fanghj@igsnr.ac.cn)

## Abstract

Accurate estimates of gross primary production (GPP) for croplands are needed to assess carbon cycle and crop yield. Satellite-based models have been developed to monitor spatial and temporal GPP patterns. However, there are still large uncertainties in estimating cropland GPP. This study compares three light use efficiency (LUE) models (MODIS-GPP, EC-LUE, and VPM) with eddy-covariance measurements at three adjacent AmeriFlux crop sites located near Mead, Nebraska, USA. These sites have different croprotation systems (continuous maize vs. maize and soybean rotated annually) and water management practices (irrigation vs. rainfed). The results reveal several major uncertainties in estimating GPP which need to be sufficiently considered in future model improvements. Firstly, the C4 crop species (maize) shows a larger photosynthetic capacity compared to the C3 species (soybean). LUE models need to use different model parameters (i.e., maximal light use efficiency) for C3 and C4 crop species, and thus, it is necessary to have accurate species-distribution products in order to determine regional and global estimates of GPP. Secondly, the 1 km sized MODIS fPAR and EVI products, which are used to remotely identify the fraction of photosynthetically active radiation absorbed by the vegetation canopy, may not accurately reflect differences in phenology between maize and soybean. Such errors will propagate in the GPP model, reducing estimation accuracy. Thirdly, the water-stress variables in the remote sensing models do not fully characterize the impacts of water availability on vegetation production. This analysis highlights the need to improve LUE models with regard to model parameters, vegetation indices, and water-stress inputs.

**Keywords:** Light use efficiency, MODIS, EC-LUE, MODIS-GPP, VPM, Maize, Soybean

Approximately, 12% of Earth's ice-free land surface is cultivated cropland (Wood et al., 2000) and up to 33% and 20% of this land surface in Europe and the United States, respectively, is arable (Ramankutty et al., 2008). Crop gross primary production (GPP) contributes approximately 15% of global carbon dioxide fixation (Malmstrom et al., 1997). There is broad agreement that global crop vegetation production is and will be significantly affected by climate change (Parry et al., 2004; Schmidhuber and Tubiello, 2007; Wheeler and von Braun, 2013). Therefore, crop vegetation production monitoring and forecasting are important for agricultural management (Mulla, 2013), food security (Meroni et al., 2014), yield estimates (Ines et al., 2013) and carbon cycle research (Gitelson et al., 2014; Li et al., 2014).

Numerous approaches have been developed to model vegetation primary production in various cropping systems (Li et al., 2013; Cai et al., 2014). Monteith (1972, 1977) remarked that throughout a wide range of crops and environmental conditions, the ratio of absorbed light to carbon assimilation over the growing season is relatively constant. Then a production efficiency model that estimated crop growth from absorbed photosynthetically active radiation (APAR) and maximal light use efficiency ( $LUE_{max}$ ) was introduced (Running et al., 2004). Subsequent studies further improved the model by expressing  $LUE_{max}$  as a function of one or more factors: light climate, temperature, water, and nutrient stress (Gamon et al., 1997; Xiao et al., 2004; Suyker and Verma, 2012).

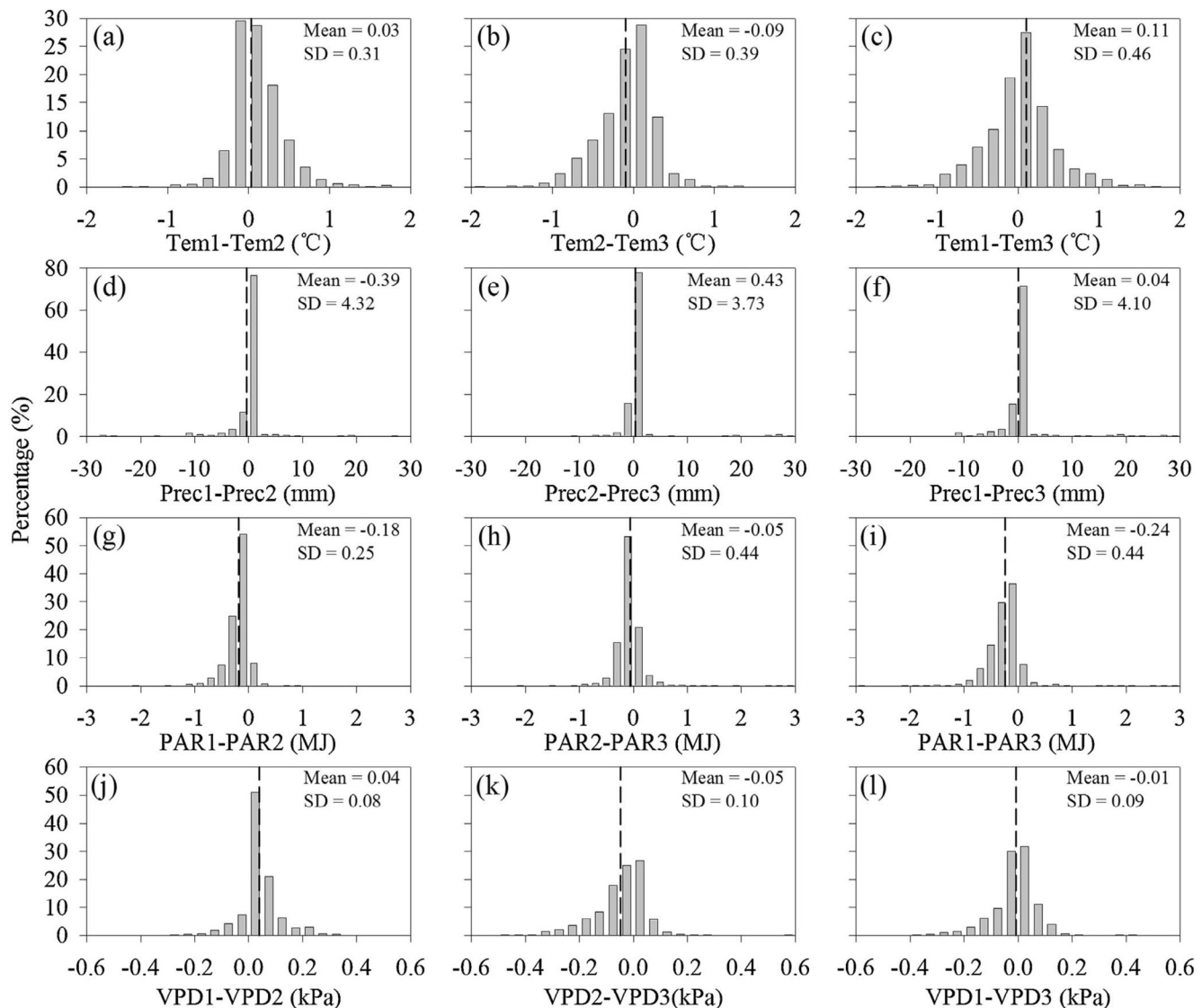


**Figure 1.** Histogram of daily difference of four climate variables among three sites. Tem, Prec, PAR and VPD indicate air temperature, precipitation, photosynthetically active radiation and vapor pressure deficit, respectively. The numbers in the x-axis label represent the site, and 1–3 represent US-NE1, US-NE2 and US-NE3, respectively. Mean and SD in the figures indicate the mean value and standard deviation of differences through all days.

However, global and regional NPP or GPP estimates of cropland ecosystems still have large uncertainties among different methods (Cramer et al., 1999). For example, carbon balance studies of European croplands have found that cropland net primary production (NPP) estimates range from 490 to 846  $\text{gCm}^{-2}\text{year}^{-1}$  using various methods (Ciais et al., 2010). Accurate estimates of vegetation production are critical as they are inputs into other models (i.e., crop yield) and can reduce the accuracy of these models. For example, crop yield estimates based on MODIS GPP data collected over the Midwestern United states were underestimated due to the absence of including the impact of irrigation (Xin et al., 2013). Even small biases in GPP models can accumulate in long-term studies and this can lead to erroneous conclusions in forecasting climate change (Richardson et al., 2012).

The goal of this study is to determine uncertainties in estimating vegetation production from MODIS imagery acquired over cropland ecosystems. These estimates will be compared with 4 years of continuous eddy covariance (EC) measurements from three AmeriFlux sites located in Nebraska, U.S.A. The specific objectives were to determine the accuracy of light use efficiency models in estimating vegetation

production by (a) crop type, maize vs. soybean, (b) water management practices, irrigated vs. rainfed, and (c) model approaches, MODIS-GPP vs. EC-LUE vs. VPM.

## 2. Models and data

### 2.1. Study sites and eddy flux measurements

In this study, three adjacent AmeriFlux eddy covariance towers were selected, which were located within 1.6km of each other at the University of Nebraska-Lincoln Agricultural Research and Development Center near Mead, Nebraska, USA. They have similar climatic conditions (Figure 1). US-Ne1 (41.1651°N, 96.4766°W) was planted as continuous maize and was equipped with a center pivot irrigation system. US-Ne2 (41.1649°N, 96.4701°W) and US-Ne3 (41.1797°N, 96.4397°W) were both planted as a maize–soybean rotation, with maize planted in odd years. Similar to US-Ne1, US-Ne2 was irrigated using center-pivot irrigation. US-Ne3 relied entirely on rainfall for moisture. The soil characterize in these three sites is very similar (Table 1). More

**Table 1.** Soil characteristics in the three study sites.

Site	Clay	Sand	SC	WP	Soil C	Soil N
US-Ne1	34.25	10.54	0.39	0.22	9.92	1.00
US-Ne2	30.35	11.84	0.41	0.26	10.16	1.06
US-Ne3	34.96	8.32	0.39	0.23	10.54	1.02

Clay: soil clay content (%); Sand: soil sand content (%); SC: field saturation moisture capacity ( $\text{m}^3 \text{m}^{-3}$ ); WP: wilting point ( $\text{m}^3 \text{m}^{-3}$ ); Soil C: soil carbon content (g/Kg); Soil N: soil nitrogen content (g/Kg).

details about the crop management and field history of these study sites are available in Suyker and Verma (2012) and Verma et al. (2005).

Flux and meteorological variables are available on the FLUXNET Synthesis Dataset (<http://www.fluxdata.org>) for these three study sites. The eddy covariance flux measurements were collected using a Gill Sonic anemometer (Model R3; Gill Instruments Ltd., Lyminster, UK), a closed-path system (LI-6262), and the LI-7500 open-path  $\text{CO}_2/\text{H}_2\text{O}$  water vapor sensor (LI-Cor Lincoln, NE). Data from the closed path system were the primary source of  $\text{CO}_2$  fluxes in these three towers, and open-path  $\text{CO}_2$  fluxes were used during the growing season only when closed-path fluxes were not available. Previous study have compared hourly  $\text{CO}_2$  fluxes measurements obtained from the closed-path and open-path system with application of WPL correction, and found, they agreed very well (Yasuda and Watanabe, 2001). Key supporting meteorological variables were measured including air temperature, humidity, incident photosynthetically active radiation, soil heat flux, incident air and soil temperature, and windspeed.

The data were quality-checked and gap-filled based on guidelines and previous studies (Munger and Loescher, 2006; Agarwal et al., 2010). Net ecosystem exchange (NEE) was processed following the FLUXNET procedure, from which GPP values were computed (Agarwal et al., 2010). Daily NEE, ecosystem respiration ( $R_e$ ), latent heat (LE), sensible heat (H), net radiation ( $R_n$ ), photosynthetically active radiation (PAR), air temperature ( $T_a$ ), daily minimum air temperature ( $T_{\min}$ ), vapor pressure deficit (VPD), and soil moisture (SWC) were collected from 2001 through 2004. GPP was calculated as the sum of NEE and  $R_e$ .

## 2.2. Light use efficiency models

### 2.2.1. EC-LUE model

Yuan et al. (2007, 2010,) developed the eddy covariance-light use efficiency (EC-LUE) model to simulate daily GPP. The EC-LUE model is driven by four variables: NDVI, PAR,  $T_a$ , and the evaporative fraction (the ratio of latent heat flux with net radiation).

$$\text{GPP} = \text{PAR} \times \text{fPAR} \times \text{LUE}_{\max} \times \text{Min}(T_s, W_s) \quad (1)$$

$$\text{fPAR} = 1.24 \times \text{NDVI} - 0.168 \quad (2)$$

$$T_s = \frac{(T_a - T_{\min}) \times (T_a - T_{\max})}{(T_a - T_{\min}) \times (T_a - T_{\max}) - (T_a - T_{\text{opt}})^2} \quad (3)$$

$$W_s = \frac{\text{LE}}{R_n} \quad (4)$$

where  $\text{LUE}_{\max}$  is the maximal light use efficiency without environmental stress ( $\text{g Cm}^{-2} \text{MJ}^{-1} \text{APAR}$ ). In the EC-LUE model, environmental stress includes water and temperature stresses. Min denotes the minimum values of  $T_s$  and  $W_s$ , assuming that the impacts of temperature and moisture on LUE follow Liebig's Law (i.e., LUE is affected only by the most limiting factor at any given time) (Liebig, 1840); and  $T_{\min}$ ,  $T_{\max}$ , and  $T_{\text{opt}}$  are the daily minimum, maximum, and optimum air temperatures ( $^{\circ}\text{C}$ ) for photosynthetic activity. If the air temperature falls below  $T_{\min}$  or increases beyond  $T_{\max}$ ,  $T_s$  is set to zero. In this study,  $T_{\min}$  and  $T_{\max}$  were set to 0 and  $40^{\circ}\text{C}$ , respectively, whereas,  $T_{\text{opt}}$  was deter-

mined using nonlinear optimization as  $21^{\circ}\text{C}$  (Yuan et al., 2007). LE is latent heat ( $\text{MJm}^{-2}$ ), and  $R_n$  is net radiation ( $\text{MJm}^{-2}$ ).

### 2.2.2. MODIS-GPP product

The MODIS-GPP algorithm (Running et al., 2004) is a LUE approach, with inputs from MODIS-fPAR, land cover, and biomespecific climatologic data sources from NASA's Data Assimilation Office. Light use efficiency is calculated based on two factors. The first is the biome-specific maximum conversion efficiency,  $\text{LUE}_{\max}$ , a multiplier that reduces the conversion efficiency when cold temperatures limit plant function. The second multiplier reduces the maximum conversion efficiency when the vapor pressure deficit (VPD) is high enough to inhibit photosynthesis. MODIS-GPP used VPD to indicate drought stress.

$$\text{GPP} = \text{PAR} \times \text{fPAR} \times \text{LUE}_{\max} \times T_s \times W_s \quad (5)$$

$$T_s = \begin{cases} 0 & T_{\min} < \text{TMIN}_{\min} \\ \frac{T_{\min} - \text{TMIN}_{\min}}{\text{TMIN}_{\max} - \text{TMIN}_{\min}} & \text{TMIN}_{\min} < T_{\min} < \text{TMIN}_{\max} \\ 1 & T_{\min} > \text{TMIN}_{\max} \end{cases} \quad (6)$$

$$W_s = \begin{cases} 0 & \text{VPD} > \text{VPD}_{\max} \\ \frac{\text{VPD}_{\min} - \text{VPD}}{\text{VPD}_{\max} - \text{VPD}_{\min}} & \text{VPD}_{\min} < \text{VPD} < \text{VPD}_{\max} \\ 1 & \text{VPD} < \text{VPD}_{\min} \end{cases} \quad (7)$$

where  $\text{TMIN}_{\max}$  is the daily minimum temperature at which  $\text{LUE} = \text{LUE}_{\max}$ ,  $\text{TMIN}_{\min}$  is the daily minimum temperature at which  $\text{LUE} = 0$ ,  $\text{VPD}_{\max}$  is the daylight average vapor pressure deficit at which  $\text{LUE} = 0$ , and  $\text{VPD}_{\min}$  is the daylight average vapor pressure deficit at which  $\text{LUE} = \text{LUE}_{\max}$ . Based on the MODIS land cover product (MOD12), a set of biome-specific radiation use efficiency parameters were extracted from the biome properties look-up table (BPLUT) for each pixel. BPLUT contains parameters for temperature and VPD limits for representative vegetation in each biome type (Running et al., 2004). Five parameters were used to calculate GPP.

### 2.2.3. VPM model

In the vegetation production model (VPM) (Xiao et al., 2004),  $\text{LUE}_{\max}$  is affected by temperature, land surface moisture, and phenology:

$$\text{GPP} = \text{PAR} \times \text{fPAR} \times \text{LUE}_{\max} \times T_s \times W_s \times P_s \quad (8)$$

fPAR is assumed to be a linear function of EVI, and the coefficient is simply set to 1.0 (Xiao et al., 2004). The  $T_s$ ,  $W_s$ , and  $P_s$  indicate the effects of temperature, water, and phenology on the light use efficiency of vegetation.  $T_s$  is estimated at each time step using the equation developed for the terrestrial ecosystem model (Raich et al., 1991) and shown in Eq. (3).

The VPM also uses the land-surface water index (LSWI) (Xiao et al., 2004) to capture the effects of water stress and phenology on plant photosynthesis:

$$\text{LSWI} = \frac{\rho_{\text{NIR}} - \rho_{\text{SWIR}}}{\rho_{\text{NIR}} + \rho_{\text{SWIR}}} \quad (9)$$

where  $\rho_{\text{NIR}}$  and  $\rho_{\text{SWIR}}$  refer to the reflectance of 841–876 nm band and 1628–1652 nm band, respectively. The water index was calculated as:

$$W_s = \frac{1 + \text{LSWI}}{1 + \text{LSWI}_{\max}} \quad (10)$$

where  $\text{LSWI}_{\max}$  is the maximum LSWI within the plant growing season for individual pixels.  $P_{\text{scalar}}$  is included to account for the effect of leaf phenology (leaf age) on photosynthesis at the canopy level as im-

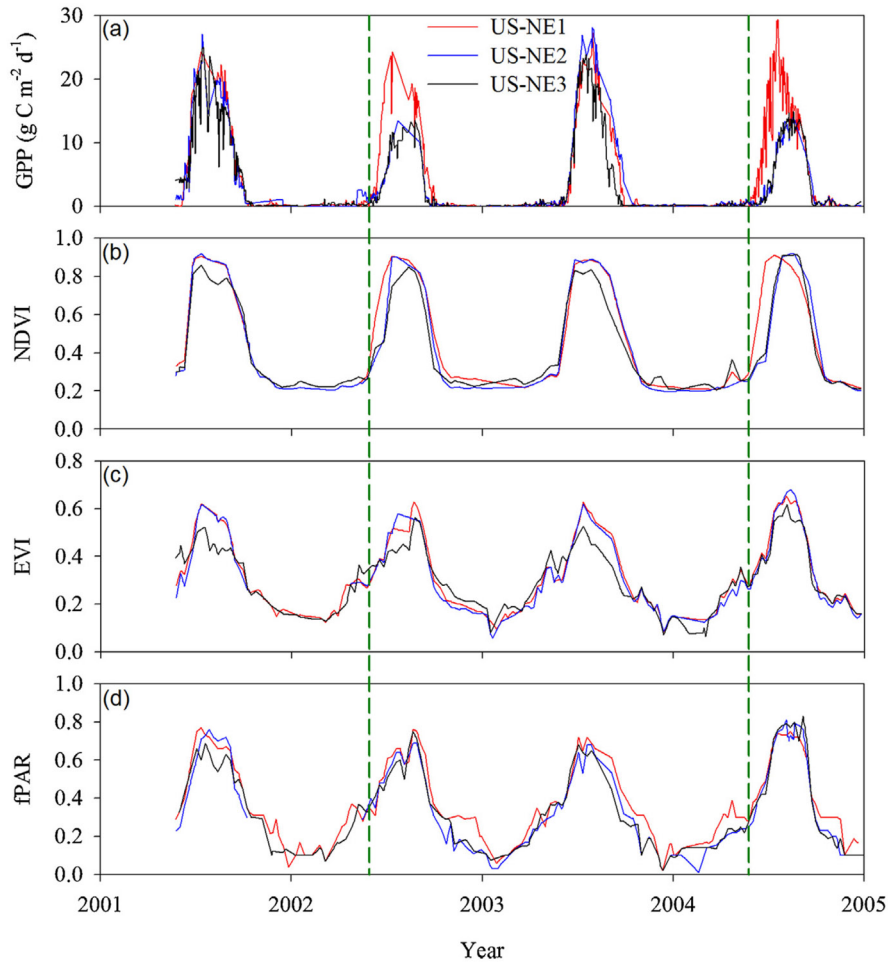


**Figure 2.** Comparison of gross primary production (GPP), normalized difference vegetation index (NDVI), enhanced vegetation index (EVI), and fraction of absorbed photosynthetically active radiation (fPAR) among the three AmeriFlux sites (US-Ne1, US-Ne2, and US-Ne3). The green dashed lines indicate the start of the maize growing season at US-Ne1 in even years.

mature leaves do not have the same photosynthetic capacity as mature leaves (Reich et al., 1991). Leaf age at the canopy level can be captured using remote sensing imagery to monitor phenological change. The calculation of  $P_s$  depends on the longevity of leaves (deciduous vs. evergreen).  $P_s$  was calculated as a linear function of LSWI from bud burst (i.e., emergence for crops) to full leaf expansion:

$$P_s = \frac{1 + \text{LSWI}}{2} \quad (11)$$

At full leaf expansion  $P_s$  was 1. The dates for the three distinct growing phases (emergence, full canopy, and senescence) were obtained using an EVI seasonal threshold similar to that of the MODIS phenology product (MOD12Q2) (Friedl et al., 2002).

### 2.3. Model operation and satellite data at the EC sites

Three LUE models were run at daily time steps at the EC sites. Environmental variables measured at the EC sites were used to drive these three models. The 16-day MODIS-NDVI/EVI data (MOD13A2) and 8-day MODIS-fPAR (MOD15A2) with 1-km spatial resolution were used to drive LUE models. Only the NDVI, EVI, and fPAR values of the pixel containing the tower were used. Quality control (QC) flags, which signal cloud contamination in each pixel, were examined to screen and reject NDVI, EVI, and fPAR data of insufficient quality. Missing or unreliable values for each 1-km MODIS pixel were tem-

porally filled in based on their corresponding quality assessment data fields as proposed by Zhao et al. (2005): (1) if the first (or last) 8-day or 16-day satellite value is unreliable or missing, it will be replaced by the closest reliable value. (2) Other unreliable values will be replaced by linear interpolation of the nearest reliable value before it and the closest reliable value after it. If there are no reliable values during the entire year, the annual maximum will be chosen from unreliable periods in the current year and will be used as a constant value across the entire year. Daily NDVI, EVI and fPAR values were derived from two consecutive 8-day or 16-day composites by linear interpretation. The daily MODIS Surface Reflectance product (MOD09GA) at 1-km spatial resolution was used to calculate LSWI. The same method that was used for NDVI was used to conduct data QC and fill missing data gaps for MODIS Surface Reflectance product.

### 2.4. Statistical methods

The nonlinear regression procedure (Proc NLIN) in the Statistical Analysis System (SAS, SAS Institute Inc., Cary, NC, USA) was applied to two calculations: (1) to conduct the statistics analysis, and (2) to optimize the parameters of three models across the study EC sites. Three metrics were used to evaluate the performance of the models, including correlation coefficient of determination ( $R_2$ ), root mean square error (RMSE), and mean predictive error (BIAS, difference between mean observations and simulations).

**Table 2.** Summary of the three light use efficiency models related to eddy covariance measurements collected at the three study sites.

	MODIS-GPP			EC-LUE			VPM		
	$R^2$	RMSE	BIAS	$R^2$	RMSE	BIAS	$R^2$	RMSE	BIAS
US-Ne1	0.65	4.91	-0.41	0.84	3.26	0.37	0.67	4.41	1.51
US-Ne2	0.67	4.52	-0.06	0.83	3.18	0.13	0.79	3.43	1.70
US-Ne3	0.64	4.17	-0.17	0.81	2.74	0.16	0.50	4.24	1.02

Units of RMSE and BIAS are  $\text{g Cm}^{-2} \text{ day}^{-1}$ .

### 3. Results

Differences in GPP estimates based on EC measurements between maize and soybean were examined for the two irrigated sites (US-Ne1 and US-Ne2), and the maximum GPP of maize was found to be substantially larger than that of soybean (Figure 2). For example, in 2004, the highest GPP of maize was  $29.20 \text{ gCm}^{-2} \text{ day}^{-1}$  (US-Ne1), but the peak value of soybean GPP was only  $13.98 \text{ gCm}^{-2} \text{ day}^{-1}$  (US-Ne2). Other environmental variables at these two sites, such as air temperature, relative humidity, photosynthetically active radiation, and soil moisture, were comparable (Figure 1). EVI and MODIS-fPAR of soybean at an irrigated site (US-Ne2) were close to those of maize at an irrigated site (US-Ne1), but there was a short lag at the start of the growing season for NDVI in soybean (Figure 2b–d).

The  $\text{LUE}_{\max}$  of MODIS, EC-LUE, and VPM was calibrated for maize and soybean, respectively.  $\text{LUE}_{\max}$  of maize was significantly larger than that of soybean ( $p < 0.05$ ) (Figure 3). For example, in the EC-LUE model,  $\text{LUE}_{\max}$  was only  $1.44 \text{ gCMJ}^{-1}$  for soybean, but  $2.25 \text{ gCMJ}^{-1}$  for maize at US-Ne2.

Uncertainties in satellite data introduce inaccuracies in GPP simulations (Figs. 4 and 5). The GPP simulations based on the MODIS-GPP and VPM models could not indicate the differences between the two crop species (Figures 4 & 5). Figure 6 shows a comparison of the ratio between GPP observations and simulations for the two sites (i.e., US-Ne1 and US-Ne2). Based on NDVI data, the ECLUE model could detect the different phenological characteristics of maize and soybean (Figure 6). However, the GPP estimates based on MODIS-GPP and VPM failed to identify the difference between the two crop species (Figure 6).

Within the three study sites, two sites were under irrigated management (US-Ne1 and US-Ne2), whereas, the third site relied entirely on rainfall (US-Ne3). Soil moisture was regulated by precipitation at the US-Ne3 site, and the average soil moisture was lower than at the two irrigated sites, (74% of that in US-Ne2; Figure 7d). This research compared the water stress variables of the three models with the observed soil moisture to investigate the differences between irrigated and rainfall-dependent sites. All the water stress variables in the three models showed lower water availability at US-Ne3 than at the US-Ne2 site (Figure 7d). However, three water variables showed large differences in identifying water stress. Both evaporative fraction (EF) and vapor pressure deficit (VPD) showed only slight decreases temporally with soil moisture at a depth of 10cm (Figure 7) and insignificant correlations with soil moisture directly (Figure 8a and b). In contrast, LSWI showed a weak correlation with soil moisture (Figure 8c).

The differences between the irrigated (US-Ne2) and rainfed site (US-Ne3) for both measured GPP and water stress variables were correlated (Figure 9). Evaporative fraction (EF) showed the highest correlation (Figure 9b) and differences in soil moisture did not explain the GPP differences between the sites (Figure 9d). Both VPD and LSWI had weak correlations in differences between the sites and measured GPP (Figure 9). Consequently, using EF as the waterstress variable, the EC-LUE model showed the best performance in simulating GPP at all three sites during the growing seasons (Table 2).

### 4. Discussion

#### 4.1. Differences of photosynthesis capability between maize and soybean

Our results imply the strong photosynthetic capacity of maize as a C4 crop type under similar climate conditions. Figure 3 shows the  $\text{LUE}_{\max}$  values of maize, are significant larger than those of soybean at all three LUE models.  $\text{LUE}_{\max}$  is an important parameter in satellite-based LUE models because it determines the expected rate of photosynthesis assuming optimal conditions. Previous studies support the conclusion that LUE models need specific model parameters for different crop species, especially for C3 and C4 species (Prince and Goward, 1995; Suyker and Verma, 2012). Yuan et al. (2010) assumed one value of  $\text{LUE}_{\max}$  for all C3 and C4 crops and found significant errors in GPP estimates. Our results illustrate a significant issue for accurate regional and global estimation of GPP: the availability of crop type-specific (i.e., C3 and C4) products is a prerequisite for model application.

#### 4.2. Impacts of vegetation index on model performance

Many LUE models depend on accurate satellite data products, which provide spatially and temporally consistent vegetation coverage information. Therefore, any noise or errors in satellite data is transferred to GPP estimates (Yuan et al., 2007). The EC-LUE and VPM models use NDVI and EVI to estimate fPAR based on linear relationships. The MODIS-GPP algorithm directly uses the MODIS-fPAR product, which uses a radiative transfer model and only employs NDVI as a back-up algorithm. There are distinct and consistent seasonal dynamics of NDVI, EVI, and fPAR during the growing season (Figure 2b–d). The growing season of maize is longer and requires earlier planting dates compared to soybean. This strongly determines the date of GPP peaks (Figure 2a). However, only NDVI clearly discriminated between maize and soybean at the start of the growing season for this data set. Both EVI and MODIS-fPAR had similar temporal behavior for both crops (Figure 2b and c).

Xiao et al. (2004) compared the correlations between the two vegetation indices (EVI, NDVI) and GPP for an evergreen needleleaf forest and found that EVI seasonal dynamics followed those of GPP better than those of NDVI in terms of GPP phase and amplitude. However, NDVI was found to be the best index to predict fPAR in subalpine grassland (Rossini et al., 2012) and is used as the back-up algorithm for estimating fPAR (Myneni et al., 1997) in the MOD15 product. In this study, differences in EVI and MODIS-fPAR between crops were not clear, and thus, were not optimal characterizing phenological stages. Figure 2 shows that both of EVI and MODIS-fPAR failed to indicate the differences of maize and soybean. This is in contrast with other studies that have determined that the behavior of EVI is linearly related to NDVI (Wardlow et al., 2007) and both VIs tend to follow each other temporally (Nguy-Robertson et al., 2013). It is possible that the EVI and fPAR products were influenced by the mixed pixels due to the high spatial resolution (1 km) which is larger than the study site (i.e.,

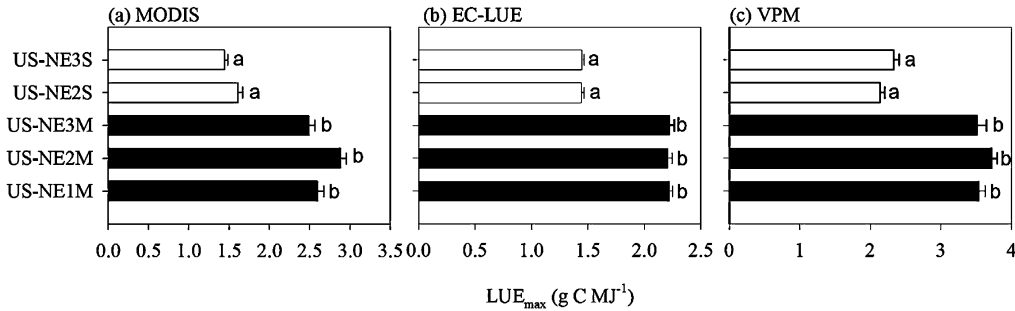


**Figure 3.** Comparison of maximal light use efficiency ( $LUE_{max}$ ) of maize and soybean at the three AmeriFlux sites (US-Ne1, US-Ne2, and US-Ne3) for MODIS-GPP (a), EC-LUE (b) and VPM (c). The “M” in the y-axis label indicates maize, and “S” indicates soybean. There was a statistical difference between the two crops for each GPP model (MODIS-GPP, EC-LUE, and VPM), indicated by ‘a’ and ‘b’. Error bars represent standard deviation of estimated parameters.

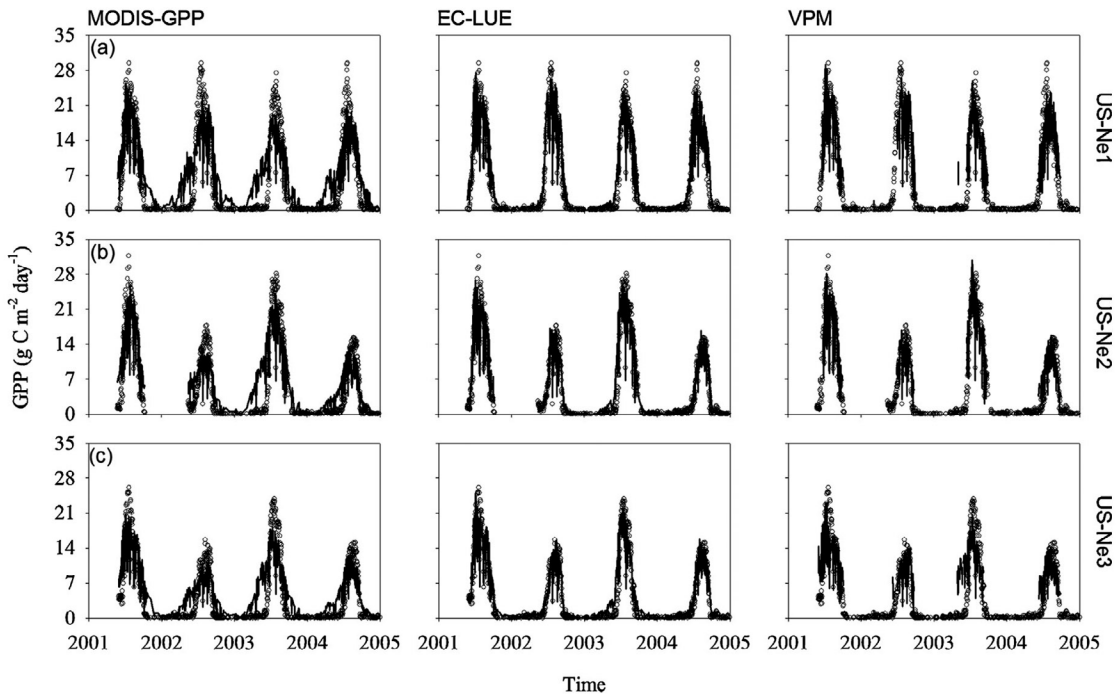


**Figure 4.** Daily variation of predicted and estimated gross primary production (GPP) from eddy covariance measurements at the three AmeriFlux sites (US-Ne1, US-Ne2, and US-Ne3). The black solid lines represent the predicted GPP from the three models (MODIS-GPP, EC-LUE, and VPM), and the open circular dots represent estimated GPP.

included roads, grass, adjacent fields). Fang et al. (2013) found that up to 71% of MODIS LAI pixels were mixed. While the Fang et al. (2013) and Lotsch et al. (2003) both determined that mixed pixels may be frequent, they do not generally impact LAI and fPAR products because surrounding vegetation has similar phenology. This assumption is not always true in crop ecosystems where the phenological behavior of surrounding vegetation may be starkly different. The temporal behavior of NDVI was likely impacted less, since it is more sensitive than EVI to low biomass and responds quickly to small changes in leaf area (Viña et al., 2011).

#### 4.3. Impacts of water stress on model performance

While multiple parameters constraining LUE have been examined, many studies have focused on different parameterizations of water stress. These different approaches have led to considerable differences in results of LUE models (Yuan et al., 2014). Defining a remote-sensing function to capture the constraint of moisture availability on plant

photosynthesis, has already been a challenge for many years. The effects of water availability on GPP have been estimated in different ways in various LUE models, including as a function of soil moisture, of evaporative fraction, and of atmospheric vapor pressure deficit (Field et al., 1995; Prince and Goward, 1995). In the EC-LUE model, water stress is estimated using the evaporative fraction (the ratio of actual evapotranspiration to net shortwave radiation) because decreasing amounts of energy devoted to evaporating water suggest a more severe moisture limitation (Kurc and Small, 2004). The VPM model uses the LSWI index to estimate the seasonal dynamics of water stress (Xiao et al., 2004).

All water-related variables used in the LUE models have uncertainties for representing water-availability constraints. Previous studies indicated that vapor pressure deficit is not a good indicator of the spatial heterogeneity of soil moisture conditions across the landscape (e.g., slopes vs. valleys) and is not likely to be linearly related to soil-water availability, for which, it is often used as a proxy (Yuan et al., 2007). In this study, the results showed slow responses of VPD to



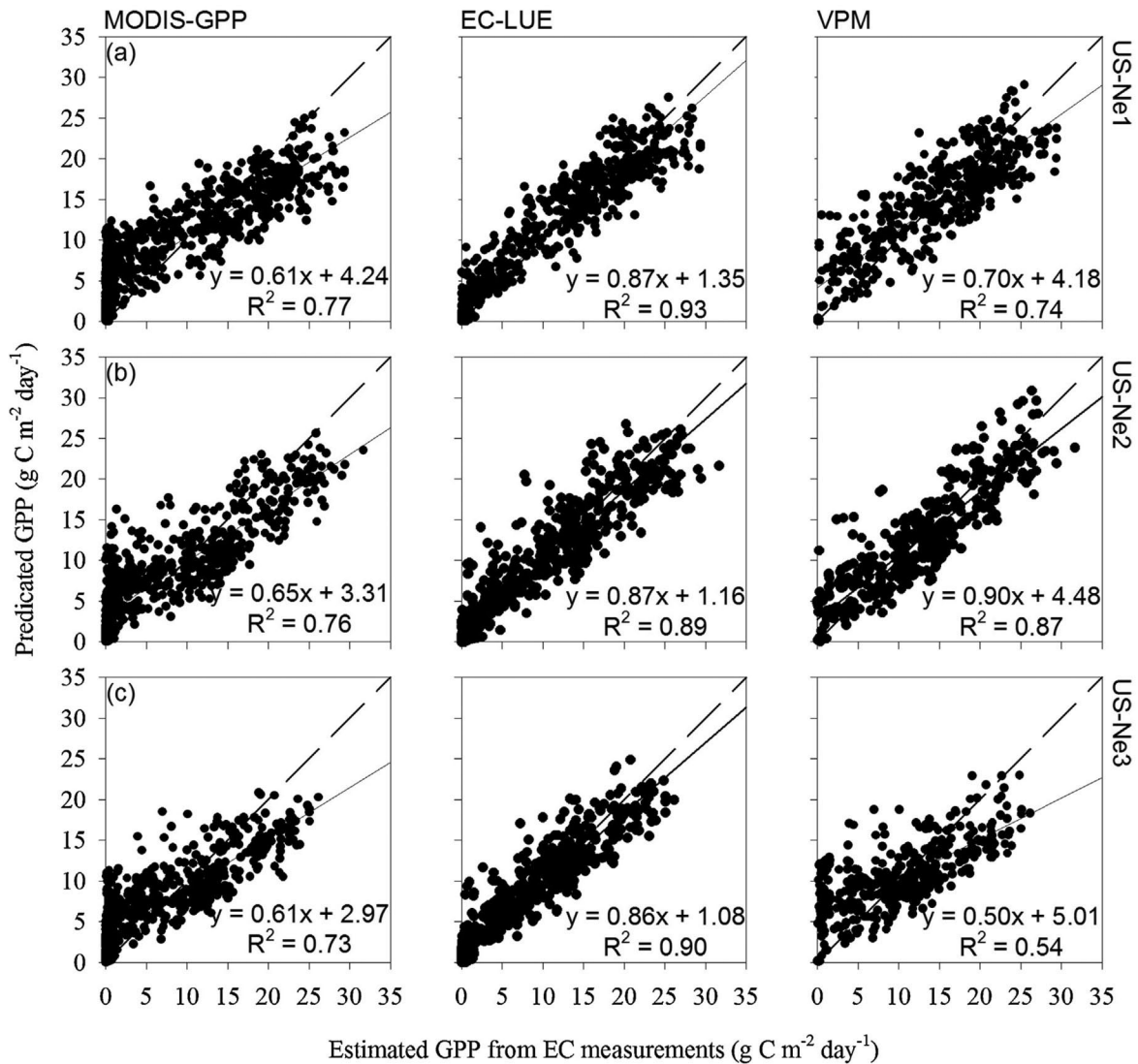


**Figure 5.** Predicted vs. the estimated GPP at the three sites. The long dash line is 1:1 line and the solid line is linear regression line.

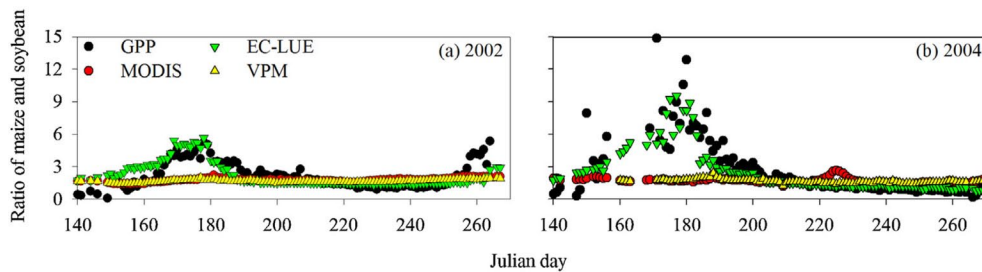


**Figure 6.** GPP ratios of maize and soybean between the AmeriFlux sites US-Ne1 and US-Ne2 for the measured and modeled (MODIS-GPP, EC-LUE, and VPM) and gross primary production (GPP).

soil moisture variations and weak correlations of differences between VPD and GPP. Although the evaporative fraction did not identify differences in soil moisture between irrigated and rainfed sites (Figure 5b), it was related to GPP differences (Figure 7b). There is a close coupling relationship between plant transpiration and photosynthesis because both water and the photosynthetic cycle exchange through the stomata (Chapin et al., 2012). Plant transpiration is the largest component of ecosystem evapotranspiration (Yuan et al., 2012; Chen et al.,

2014). However, the evaporative fraction needs an ET model to simulate ecosystem evapotranspiration, and there are still large uncertainties in the current ET models (Chen et al., 2014). Any noises or errors in the ET simulations, therefore, would have been transferred to GPP predictions and further reduce LUE model performance (Yuan et al., 2014). Although the LSWI was sensitive to soil moisture variability (Figure 6c), the differences between the two sites in both LSWI and GPP were only weakly correlated (Figure 7c).

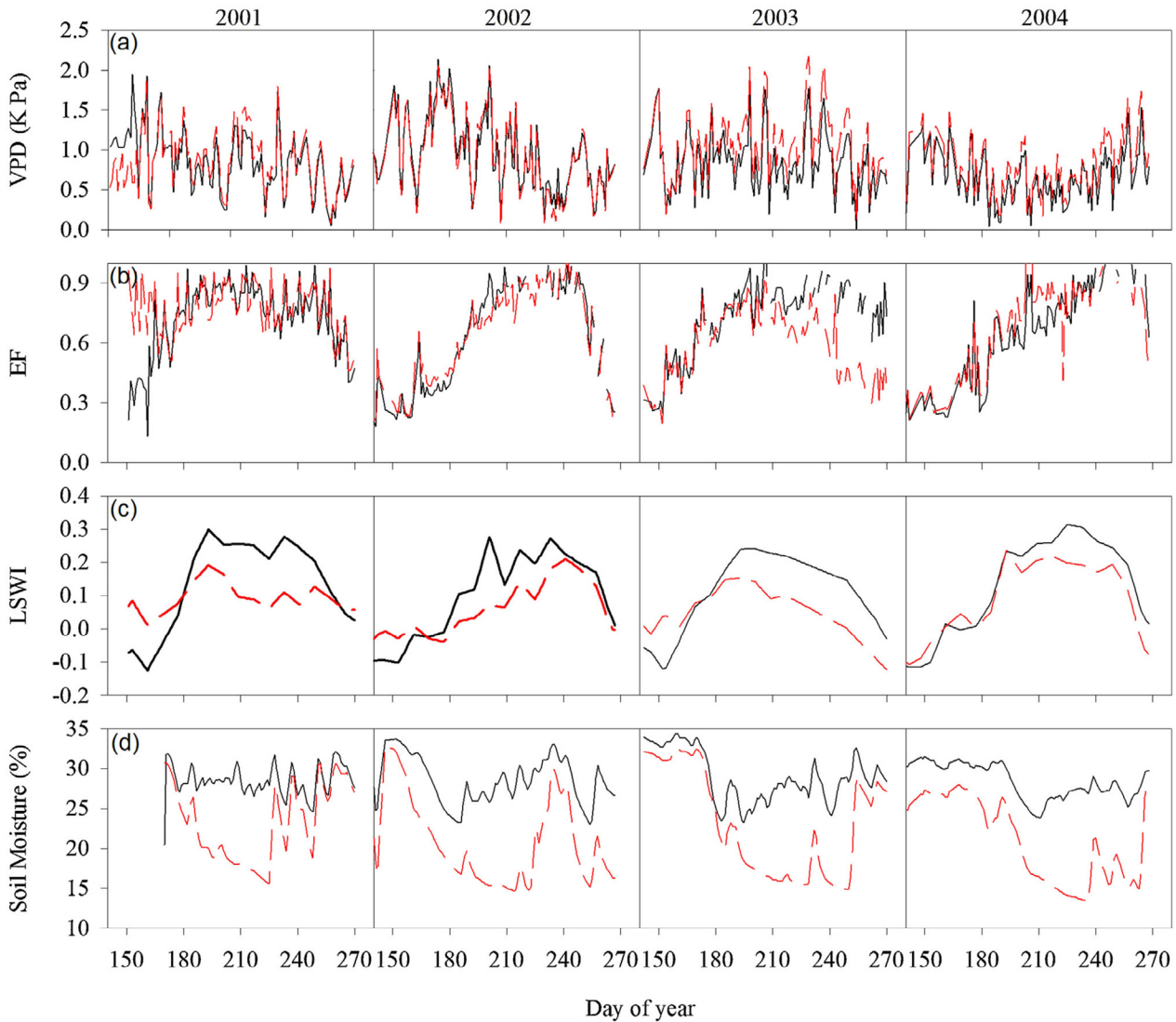


**Figure 7.** Three water-stress variables (vapor pressure deficit, VPD; evaporative fraction, EF; and land surface water index, LSWI) at the irrigated (US-Ne2, solid black line) and the rainfed sites (US-Ne3, dashed red line).

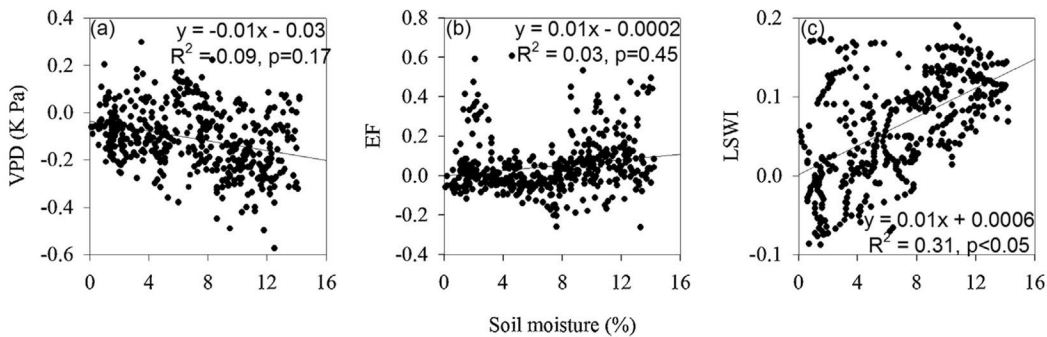


**Figure 8.** Correlation of the differences of three water-stress variables (vapor pressure deficit, VPD; evaporative fraction, EF; and land surface water index, LSWI) and soil moisture between the irrigated (US-Ne2) and the rainfed sites (US-Ne3). The coefficient of determination ( $R^2$ ) for the best-fit line was indicated.

Water availability is the dominant control for most terrestrial ecosystems (Yuan et al., 2007), and previous studies have reported that rainfed cropland accounts for 72% of cropland globally (FAO, 2005). Recent increases in global drought incidence (Dai et al., 2004) and decreased in global evapotranspiration suggest that current terrestrial

ecosystems are finding themselves in more water-limited environments (Jung et al., 2010). However, our results showed that it remains difficult to characterize water availability for plants and its effect on photosynthesis, and this limits the accuracy of GPP models. Further research on the effects of water stress is still necessary.

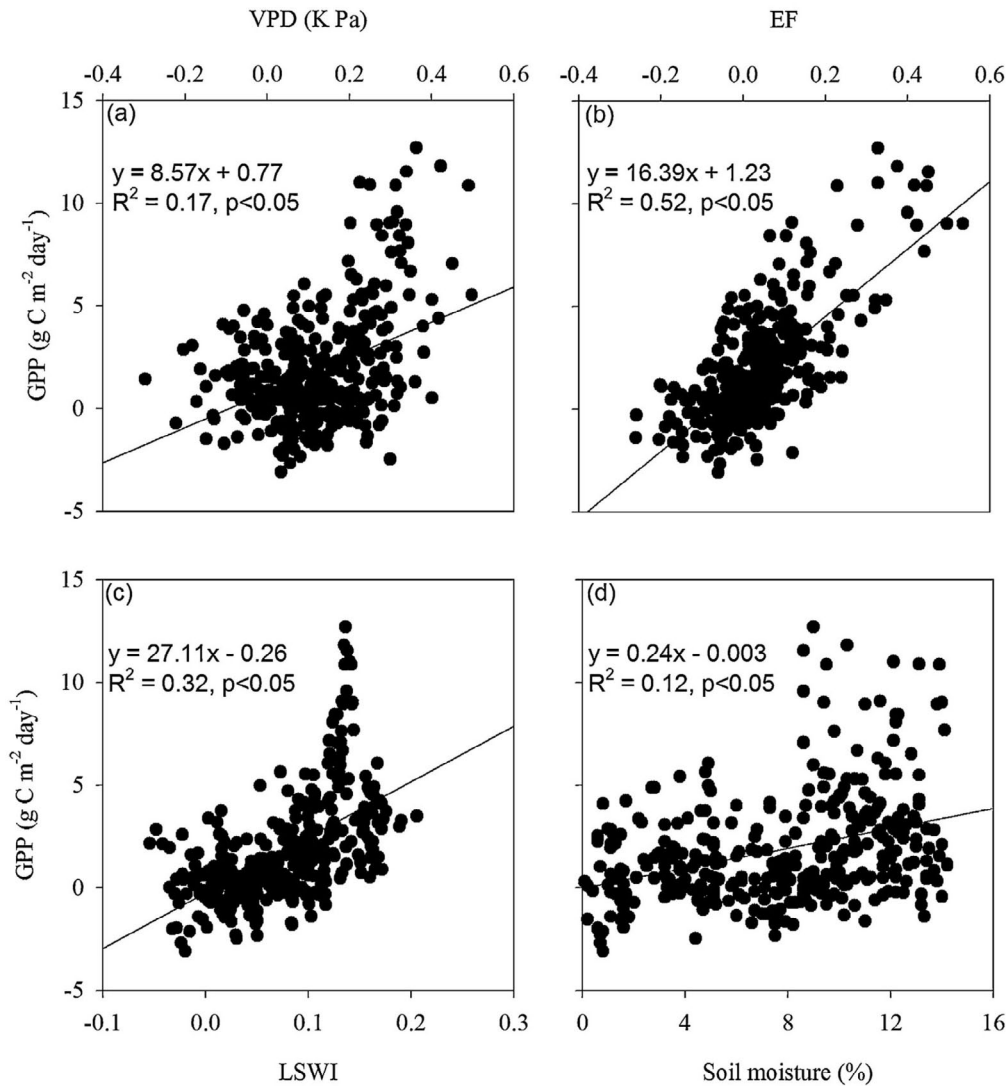


**Figure 9.** Correlation of the differences of water-stress variables and gross primary production (GPP) between the irrigated (US-Ne2) and rainfed sites (US-Ne3).

### Summary

Three light use efficiency models (MODIS-GPP, EC-LUE, and VPM) were examined at three adjacent sites with different crop species (maize and soybean) and management practices (irrigated and rainfed). Because of their differences in photosynthesis capability, GPP estimation algorithms are species-specific for maize and soybeans in all three models, which highlights the availability of crop-specific (i.e., C3 and C4) distribution products for accurately estimating regional and global GPP of cropland. Moreover, the results showed maize has an earlier growing season than soybean, but EVI and MODIS-fPAR for the study sites could not accurately identify the associated phenological differences, resulting in large model errors. The analyses conducted in this research indicate that the model water stress equations are limited in their ability to determine the impacts of water availability on vegetation production. Although the LSWI was sensitive to soil moisture variability, differences between the two sites in both LSWI and GPP were only weakly correlated.

**Acknowledgments** — This study was supported by the National Science Foundation for Excellent Young Scholars of China (41322005), the National

High Technology Research and Development Program of China (863 Program) (2013AA122003) and Program for New Century Excellent Talents in University (NCET-12-0060).

### References

- Agarwal, D.A., Humphrey, M., Beekwilder, N.F., Jackson, K., Goode, M., Van Ingen, C., 2010. A data-centered collaboration portal to support global carbon-flux analysis. *Concurrency Comput. Pract. Exper.* 22, 2323–2334.
- Cai, W.W., Yuan, W.P., Liang, S.L., Zhang, X.T., Dong, W.J., Xia, J.Z., Fu, Y., Chen, Y., Liu, D., Zhang, Q., 2014. Improved estimations of gross primary production using satellite-derived photosynthetically active radiation. *J. Geophys. Res.: Biogeosci.* 119, 110–123.
- Chapin, F.S., Matson, P.A., Vitousek, P., Chapin, M.C., 2012. *Principles of Terrestrial Ecosystem Ecology*. Springer, New York, NY.
- Chen, Y., Xia, J.Z., Liang, S.L., Feng, J.M., Fisher, J.B., Li, X., Li, X.L., Liu, S.G., Ma, M.G., Miyata, A., Mu, Q.Z., Sun, L., Tang, J.W., Wang, K.C., Wen, J., Xue, Y.J., Yu, G.R., Zha, T.G., Zhang, L., Zhang, Q., Zhao, T.B., Zhao, L., Yuan, W.P., 2014. Comparison of evapotranspiration models over terrestrial ecosystem in China. *Remote Sens. Environ.* 140, 279–293.
- Ciais, P., Wattenbach, M., Vuichard, N., Smith, P., Piao, S.L., Don, A., Luysaert, S., Janssens, I.A., Bondeau, A., Dechow, R., Leip, A., Smith, P.C., Beer, C.,

- van der Werf, G.R., Gervois, S., Vanoost, K., Tomelleri, E., Freibauer, A., Schulze, E.D., Carboneurope Synthesis Team, 2010. The European carbon balance: Part2: Croplands. *Global Change Biol.* 16, 1409–1428.
- Cramer, W., Kicklighter, D.W., Bondeau, A., Moore, B., Churkina, C., Nemry, B., Ruimy, A., 1999. Comparing global models of terrestrial net primary productivity NPP: Overview and key results. *Global Change Biol.* 5, 1–15.
- Dai, A., Trenberth, K.E., Qian, T., 2004. A global data set of Palmer drought severity index for 1870–2002: relationship with soil moisture and effects of surface warming. *J. Hydrometeorol.* 5, 1117–1130.
- Fang, H., Li, W., Myneni, R.B., 2013. The impact of potential land cover misclassification on MODIS leaf area index (LAI) estimation: A statistical perspective. *Remote Sens.* 5, 830–844.
- Field, C.B., Jackson, R.B., Mooney, H.A., 1995. Stomatal responses to increased CO<sub>2</sub>: Implications from the plant to the global scale. *Plant Cell Environ.* 18, 1214–1225.
- Food Agriculture Organization of the United Nations (FAO), 2005. FAO Statistical Databases (FAOSTAT). <http://faostat.fao.org/>
- Friedl, M.A., McIver, D.K., Hodges, J.C.F., Zhang, X.Y., Muchoney, D., Strahler, A.H., Woodcock, C.E., Gopal, S., Schneider, A., Cooper, A., Bacchini, A., Gao, F., Schaaf, C., 2002. Global land cover mapping from MODIS: Algorithms and early results. *Remote Sens. Environ.* 83, 287–302.
- Gamon, J.A., Serrano, L., Surfus, J.S., 1997. The photochemical reflectance index: an optical indicator of photosynthetic radiation use efficiency across species, functional types, and nutrient levels. *Oecologia* 112 (4), 492–501.
- Gitelson, A.A., Peng, Y., Arkebauer, T.J., Schepers, J., 2014. Relationships between gross primary production, green LAI, and canopy chlorophyll content in maize: Implications for remote sensing of primary production. *Remote Sens. Environ.* 144, 65–72.
- Ines, A.V.M., Das, N.N., Hansen, J.W., Njoku, E.G., 2013. Assimilation of remotely sensed soil moisture and vegetation with a crop simulation model for maize yield prediction. *Remote Sens. Environ.* 138, 149–164.
- Jung, M., Reichstein, M., Ciais, P., Seneviratne, S.I., Sheffield, J., Goulden, M.L., Bonan, G., Cescatti, A., Chen, J.Q., de Jeu, R., Dolman, A.J., Eugster, W., Gerten, D., Gianelle, D., Gobron, N., Heinke, J., Kimball, J., Law, B.E., Montagnani, L., Mu, Q.Z., Mueller, B., Oleson, K., Papale, D., Richardson, A.D., Rouspard, O., 2010. Recent decline in the global land evapotranspiration trend due to limited moisture supply. *Nature* 467, 951–954.
- Kurc, S.A., Small, E.E., 2004. Dynamics of evapotranspiration in semiarid grassland and shrubland ecosystems during the summer monsoon season, central New Mexico. *Water Resour. Res.* 40, W09305.
- Liebig, J., 1840. *Chemistry and Its Application to Agriculture and Physiology*. Taylor and Walton, London.
- Li, X.L., Liang, S.L., Yu, G.R., Yuan, W.P., Cheng, X., Xia, J.Z., Zhao, T.B., Feng, J.M., Ma, Z.G., Ma, M.G., Liu, S.M., Chen, J.Q., Shao, C.L., Li, S.G., Zhang, X.D., Zhang, Z.Q., Chen, S.P., Ohta, T., Varlagin, A., Miyata, A., Takagi, K., Saiqusa, N., Kato, T., 2013. Estimation of gross primary production over the terrestrial ecosystems in China. *Ecol. Model.* 261–262, 80–92.
- Li, Z., Liu, S., Tan, Z., Bliss, N., Young, C.J., West, T.O., Ogle, S., 2014. Comparing cropland net primary production estimates from inventory, a satellite-based model, and a process-based model in the Midwest of the United States. *Ecol. Model.* 277, 1–12.
- Lotsch, A., Tian, Y., Friedl, M.A., Myneni, R.B., 2003. Land cover mapping in support of LAI and FAPAR retrievals from EOS-MODIS and MISR: Classification methods and sensitivities to errors. *Int. J. Remote Sens.* 24, 1997–2016.
- Malmstrom, C.M., Thompson, M.V., Juday, G.P., Los, S.O., Randerson, J.T., Field, C.B., 1997. Interannual variation in global-scale net primary production: Testing model estimates. *Global Biogeochem. Cycles* 11, 367–392.
- Meroni, M., Verstraete, M.M., Rembold, F., Urbano, F., Kayitakire, F., 2014. A phenology-based method to derive biomass production anomalies for food security monitoring in the Horn of Africa. *Int. J. Remote Sens.* 35, 2472–2492.
- Monteith, J.L., 1972. Solar radiation and productivity in tropical ecosystems. *J. Appl. Ecol.* 9, 744–766.
- Monteith, J.L., 1977. Climate and the efficiency of crop production in Britain. *Philos. Trans. R. Soc. London A* 281, 277–294.
- Mulla, D.J., 2013. Twenty five years of remote sensing in precision agriculture: Key advances and remaining knowledge gaps. *Biosyst. Eng.* 114, 358–371.
- Munger, J.W., Loesch, H.W., 2006. Guidelines for Making Eddy Covariance Flux Measurements, <http://public.ornl.gov/ameriflux/sop.shtml/> (Nov. 29, 2011)
- Myneni, R.B., Ramakrishna, R., Nemani, R., Running, S.W., 1997. Estimation of global leaf area index and absorbed par using radiative transfer models. *IEEE Trans. Geosci. Remote Sens.* 35, 1380–1393.
- Nguy-Robertson, A., Gitelson, A., Peng, Y., Walter-Shea, E., Leavitt, B., Arkebauer, T., 2013. Continuous monitoring of crop reflectance, vegetation fraction, and identification of developmental stages using a four band radiometer. *Agron. J.* 105, 1769–1779.
- Parry, M.L., Rosenzweig, C., Iglesias, A., Livermore, M., Fischer, G., 2004. Effects of climate change on global food production under SRES emissions and socio-economic scenarios. *Global Environ. Change A* 14, 53–67.
- Prince, S.D., Goward, S.N., 1995. Global primary production: A remote sensing approach. *J. Biogeogr.* 22, 815–835.
- Raich, J.W., Rastetter, E.B., Melillo, J.M., Kicklighter, D.W., Steudler, P.A., Peterson, B.J., Grace, A.L., Moore, B., Vorosmarty, C.J., 1991. Potential net primary productivity in South America: Application of a global model. *Ecol. Appl.* 1, 399–429.
- Ramankutty, N., Evan, A.T., Monfreda, C., Foley, J.A., 2008. Farming the planet: 1. Geographic distribution of global agricultural lands in the year 2000. *Global Biogeochem. Cycles* 22, GB1003.
- Reich, P.B., Walters, M.B., Ellsworth, D.S., 1991. Leaf age and season influence the relationships between leaf nitrogen leaf mass per area and photosynthesis in maple and oak trees. *Plant Cell Environ.* 14, 251–259.
- Richardson, A.D., Anderson, R.S., Arain, M.A., Barr, A.G., Bohrer, G., Chen, G.S., Chen, J.M., Ciais, P., Davis, K.J., Desai, A.R., Dietze, M.C., Dragoni, D., Garrity, S.R., Gough, C.M., Grant, R., Hollinger, D.Y., Margolis, H.A., McCaughey, H., Migliavacca, M., Monson, R.K., Munger, J.W., Poulter, B., Raczka, B.M., Ricciuto, D.M., Sahoo, A.K., Schaefer, K., Tian, H.Q., Vargas, R., Verbeeck, H., Xiao, J.F., Xue, Y.K., 2012. Terrestrial biosphere models need better representation of vegetation phenology: Results from the North American Carbon Program Site Synthesis. *Global Change Biol.* 18, 566–584.
- Rossini, M., Cogliati, S., Meroni, M., Migliavacca, M., Galvagno, M., Busetto, L., Cremonese, E., Julitta, T., Siniscalco, C., di Cella, U.M., Colombo, R., 2012. Remote sensing-based estimation of gross primary production in a sub-alpine grassland. *Biogeosciences* 9, 2565–2584.
- Running, S.W., Nemani, R.R., Heinsch, F.A., Zhao, M., Reeves, M., Hashimoto, H., 2004. A continuous satellite-derived measure of global terrestrial primary production. *Biosciences* 546, 547–560.
- Schmidhuber, J., Tubiello, F.N., 2007. Global food security under climate change. *Proc. Natl. Acad. Sci. U. S. A.* 104, 19703–19708.
- Suyker, A.E., Verma, S.B., 2012. Gross primary production and ecosystem respiration of irrigated and rainfed maize–soybean cropping systems over 8 years. *Agric. For. Meteorol.* 165, 12–24.
- Verma, S.B., Dobermann, A., Cassman, K.G., Walters, D.T., Knops, J.M., Arkebauer, T.J., Suyker, A.E., Burba, G.G., Amos, B., Yang, H.S., Ginting, D., Hubbard, K.G., Gitelson, A.A., Walter-Shea, E.A., 2005. Annual carbon dioxide exchange in irrigated and rainfed maize-based agroecosystems. *Agric. For. Meteorol.* 131, 77–96.
- Viña, A., Gitelson, A.A., Nguy-Robertson, A.L., Peng, Y., 2011. Comparison of different vegetation indices for the remote assessment of green leaf area index of crops. *Remote Sens. Environ.* 115 (12), 3468–3478.
- Wardlow, B.D., Egbert, S.L., Kastens, J.H., 2007. Analysis of time-series MODIS 250m vegetation index data for crop classification in the U.S. Central Great Plains. *Remote Sens. Environ.* 108, 290–310.
- Wheeler, T., von Braun, J., 2013. Climate change impacts on global food security. *Science* 341, 508–513.

- Wood, S., Sebastian, K., Scherr, S.J., 2000. Pilot Analysis of Global Ecosystems (Agroecosystems), 110. International Food Policy Research Institute and World Resources Institute, Washington, DC.
- Xiao, X.M., Zhang, Q.Y., Braswell, B., Urbanski, S., Boles, S., Wofsy, S., Moore III, B., Ojima, D., 2004. Modeling gross primary production of temperate deciduous broadleaf forest using satellite images and climate data. *Remote Sens. Environ.* 912, 256–270.
- Xin, Q.C., Gong, P., Yu, C.Q., Yu, L., Broich, M., Suyker, A.E., Myneni, R.B., 2013. A production efficiency model-based method for satellite estimates of corn and soybean yields in the Midwestern US. *Remote Sens.* 5, 5926–5943.
- Yasuda, Y., Watanabe, T., 2001. Comparative measurements of CO<sub>2</sub> flux over a forest using closed-path and open-path CO<sub>2</sub> analysers. *Boundary-Layer Meteorol.* 100, 191–208.
- Yuan, W.P., Cai, W.W., Xia, J.Z., Chen, J., Liu, S., Dong, W., Merbold, L., Law, B., Arain, M.H., Beringer, J., Bernhofer, C., Black, A., Blanken, P.D., Cescaatti, A., Chen, Y., Francois, L., Gianelle, D., Janssens, I.A., Jung, M., Kato, T., Kiely, G., Liu, D., Marcolla, B., Montagnani, L., Raschi, A., Rouspard, O., Varlagin, A., Wohlfahrt, G., 2014. Comparison of light use efficiency models for simulating global terrestrial vegetation gross primary production based on the LaThuile database. *Agric. For. Meteorol.* 192–193, 108–120.
- Yuan, W.P., Liu, S.G., Liang, S.L., Tan, Z.X., Liu, H.P., Young, C., 2012. Estimations of evapotranspiration and water balance with uncertainty over the Yukon River Basin. *Water Resour. Manage.* 26, 2147–2157.
- Yuan, W.P., Liu, S., Yu, G., Bonnefond, J.-M., Chen, J., Davis, K., Desai, A.R., Goldstein, A.H., Gianelle, D., Rossi, F., Suyker, A.E., Verma, S.B., 2010. Global estimates of evapotranspiration and gross primary production based on MODIS and global meteorology data. *Remote Sens. Environ.* 114, 1416–1431.
- Yuan, W.P., Liu, S.G., Zhou, G.S., Zhou, G.Y., Tieszen, L.L., Baldocchi, D., Bernhofer, C., Gholz, H., Goldstein, A.H., Goulden, M.L., Hollinger, D.Y., Hu, Y., Lawn, B.E., Stoy, P.C., Vesala, T., Wofsy, S.C., 2007. Deriving a light use efficiency model from eddy covariance flux data for predicting daily gross primary production across biomes. *Agric. For. Meteorol.* 1433, 189–207.
- Zhao, M., Heinsch, F.A., Nemani, R., Running, S.W., 2005. Improvements of the MODIS terrestrial gross and net primary production global data set. *Remote Sens. Environ.* 95, 164–176.